Longitudinally unzipped carbon nanotubes for supercapacitors

Young Soo Yun and Hyoung-Joon Jin*

Department of Polymer Science and Engineering,
Inha University,
402-751 Incheon, Korea
Fax: +82-32-865-5178
E-mail: promars0soo@gmail.com
E-mail: hjjin@inha.ac.kr
*Corresponding author

Abstract: In this study, longitudinally unzipped carbon nanotubes (L-UCNTs) prepared from multiwalled carbon nanotubes and their electrochemical properties for supercapacitors were investigated after thermal treatment. Thermally treated L-UCNTs (RL-UCNTs) had a specific surface area of 288 m^2/g and mesoporous pore characteristics. Also, RL-UCNTs had numerous oxygen heteroatoms, which affected electrochemical performances of RL-UCNTs. RL-UCNTs exhibited a specific capacitance of 106 F/g and cycle stabilities over 5000 repetitive cycles.

Keywords: carbon nanotubes; electrode; supercapacitor; nanoribbon; transmission microscopy; X-ray photoelectron spectroscopy; nitrogen adsorption and desorption method.

Reference to this paper should be made as follows: Yun, Y.S. and Jin, H-J. (2014) 'Longitudinally unzipped carbon nanotubes for supercapacitors', *Int. J. Nanotechnol.*, Vol. 11, Nos. 5/6/7/8, pp.434–440.

Biographical notes: Young Soo Yun is currently a post doctoral researcher of Materials Science and Engineering in Seoul National University (Seoul, South Korea). He did his PhD (2013) in the Department of Polymer Science and Engineering, Inha University (Incheon, South Korea), where he received Master's degree (2010) and BA (2007). His research interests include synthesis and applications of carbon materials for energy storage systems.

Hyoung-Joon Jin is currently a Professor of Polymer Science and Engineering in Inha University (Incheon, South Korea), where he received the PhD (2000), Master's degree (1996) and BA (1994). From 2001 to 2003, he was a postdoctoral fellow of Chemical & Biological Engineering in Tufts University (USA), where he started to work in the field of natural polymers for medical applications with Professor D.L. Kaplan. His main research interests are in nanostructured carbons for energy storage and conversion, and nanofabrication of polymeric materials and biopolymers, especially silk fibroins and bacterial celluloses, for electronic devices. His group has published over 110 SCI journal papers since 2003.

1 Introduction

Supercapacitors have attracted much attention for their high power capabilities, good reversibility, and long cycle life [1,2]. Supercapacitors based on electrochemical double layer capacitance store and release energy by nanoscopic charge separation at the electrochemical interface between an electrode and an electrolyte. As the energy stored is inversely proportional to the thickness of the double layer, these capacitors have an extremely high energy density compared to conventional dielectric capacitors. The electrochemical performances of supercapacitors are determined mainly by electrodes, and therefore, various nanoscale carbon materials have been applied as an electrode material for supercapacitors [3–8].

Graphene, a new class of two-dimensional carbon nanostructure, has attracted considerable attention owing to its unique physical, chemical, and mechanical properties, such as high mechanical strength (>1060 GPa), high thermal conductivity (~3000 W/m K), high mobility (15,000 cm^2/V s), and high specific surface area (2600 m^2/g) [9–11]. Thin, elongated strips of graphene that possess straight edges, referred to as graphene nanoribbons, gradually transform from semiconductors to semimetals as their width increases, and represent a particularly versatile variety of grapheme [12,13]. Making graphene nanoribbon using lithographic, chemical, or sonochemical methods is challenging [14–16]. However, Kosynkin et al. recently reported longitudinally unzipped carbon nanotubes (L-UCNTs) to form graphene nanoribbons [17]. The method is accessible, and opens opportunities for several applications using the L-UCNTs. Nevertheless, there have been no reports for supercapacitor electrodes using L-UCNTs. Unzipping of carbon nanotubes (CNTs) result in a great change of characteristics in CNTs. Especially, L-UCNTs have increased edge sites compared to CNTs, which could bring about different surface properties. Also, L-UCNTs have different morphologies and electrical properties compared to graphene oxide [17]. Therefore, what characterises electrochemical properties of L-UCNTs is meaningful for expansion of their applications.

In this study, we prepared L-UCNTs and thermally treated L-UCNTs to make reduced L-UCNTs with increased electrical properties. The reduced L-UCNTs (RL-UCNTs) were tested as an electrode for supercapacitors. RL-UCNTs had mesoporous pore characteristics, and numerous oxygen heteroatoms. And their electrochemical performances were greatly affected by the oxygen functional groups.

2 Experimental

2.1 Preparation of RL-UCNTs

The L-UCNTs were prepared according to a previous report [17]. Specifically, 200 mg of multiwalled CNTs (MWCNTs, NCT, Japan) were suspended in concentrated 200 ml of H_2SO_4 for 6 h. 1 g of $KMnO_4$ was then added and the mixture allowed to stir for 1 h at room temperature. The reaction was then heated in an oil bath at 55°C for 30 min and then the temperature was increased to 70°C and stabilised for 1 h. After the reaction was completed, the reactant was poured onto 400 ml of ice containing 50 ml of 30% H_2O_2. After vacuum filtration for washing with ether and ethanol, the solid was ultrasound-treated in 150 ml of distilled water. Then, the aqueous suspension was frozen in liquid

nitrogen and then freeze-dried using a lyophiliser (LP3, Jouan, France) at -50°C and 0.045 mbar for 72 h [11]. After lyophilisation, low density, loosely packed L-UCNTs were thermally treated in a tubular furnace from room temperature to 600°C, using a heating rate of 10°C/min and an Ar flow rate of 200 ml/min. The thermal treatment was performed for 2 h at this temperature (600°C). Then, the resultant product was stored in a vacuum oven at 30°C.

2.2 Characterisation

The morphologies of L-UCNTs were characterised by field emission transmission electron microscopy (FE-TEM, JEM2100F, JEOL, Japan). X-ray photoelectron spectroscopy (XPS, PHI 5700 ESCA) was performed using monochromated Al Kα radiation (hν = 1486.6 eV). The porous properties of the RL-UCNTs were analysed using nitrogen adsorption and desorption isotherms that were obtained using the surface area and a porosimetry analyser (ASAP 2020, Micromeritics, USA) at –196°C. The Brunauer-Emmett-Teller (BET) surface areas (SBET) were calculated according to BET theory. The electrodes for the electrochemical tests were prepared as follows. The samples and polytetrafluoroethylene as a binder were mixed with a mass ratio of 9 : 1, coated onto a nickel mesh substrate (1×1 cm^2), and dried at 110°C for several hours. Each electrode contained about 3–4 mg of the electroactive materials. All electrochemical measurements were performed in a three-electrode system. The samples containing nickel mesh, platinum plate, and saturated KCl were used as the working, counter, and reference electrodes, respectively. The measurements were carried out in a 1 M H_2SO_4 solution at room temperature by a potentiostat/galvanostat (Autolab, PGSTAT302N, Netherlands). Cyclic voltammetry (CV) tests were performed between 0 V and 1 V (vs. SCE) at a scan rate of 20 mV/s. Galvanostatic charge/discharge results were obtained in the potential window of 0–1 V at different current densities. The capacitance retentions were investigated at a scan rate of 50 mV/s for 5000 cycles.

3 Results and discussion

As shown in Figure 1, nanoribbons were prepared from MWCNTs with a starting diameter of about 50 nm [18]. After reaction, the width of the carbon nanostructures increased to about 100 nm and their lengths were maintained to several micrometers.

The surface functional groups of L-UCNTs and RL-UCNTs were analysed by XPS (Figure 2). In the C 1*s* spectra of L-UCNTs, several distinct peaks (C-O and C(O)O centred at 286.8 and 287.7 eV, respectively) were exhibited including the main C-C peak at 284.7 eV (Figure 2(a)). Also, the two distinct peaks (532.6 and 533.1 eV) in the O 1*s* spectra revealed the presence of oxygen atoms in the carbonyl groups and various other oxygen groups such as epoxy and hydroxyl groups (Figure 2(c)). The oxygen contents of L-UCNTs were 31.0 at%. These results indicate that L-UCNTs are fully oxidised, and their surface properties are similar to graphene oxide [11]. However, graphene nanoribbons have more edge sites compared to graphene oxide. Therefore, more oxygen functional groups could be introduced on the edge site of graphene nanoribbon. After thermal treatment, in the C 1*s* spectra of RL-UCNTs, intensities of the C-O and C(O)O peaks centred at 285.4 and 289.5 eV, respectively were greatly decreased

(Figure 2(b). The oxygen contents of RL-UCNTs were decreased to 14.5 at%. However, in the O 1*s* spectra of RL-UCNTs, the two distinct peaks (530.5 and 532.5 eV) were similarly exhibited compared to L-UCNTs. During the thermal reduction process, L-UCNTs are expected to undergo structural changes. The carbon atoms in the basal plane may rearrange during annealing due to the available thermal energy. The C-O bonds in RL-UCNTs could be different from them of L-UCNTs, and mainly composed of thermo-stable ether groups (532.5 eV). And also, the carbonyl groups of L-UCNTs could be rearranged to more thermo-stable configurations (530.5 eV) [19].

Figure 1 TEM images of L-UCNTs with different magnifications

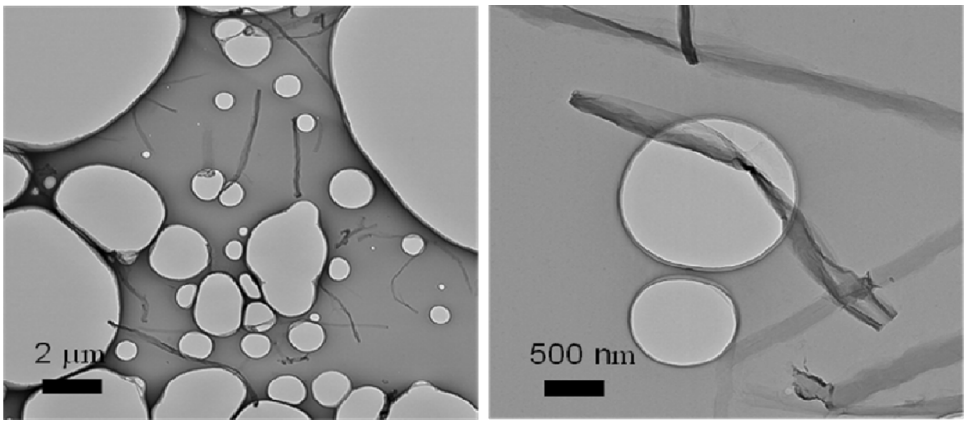

Figure 2 XPS C 1s spectra of (a) L-UCNTs and (b) RL-UCNTs, and XPS O 1s spectra of (c) L-UCNTs and (d) RL-UCNTs (see online version for colours)

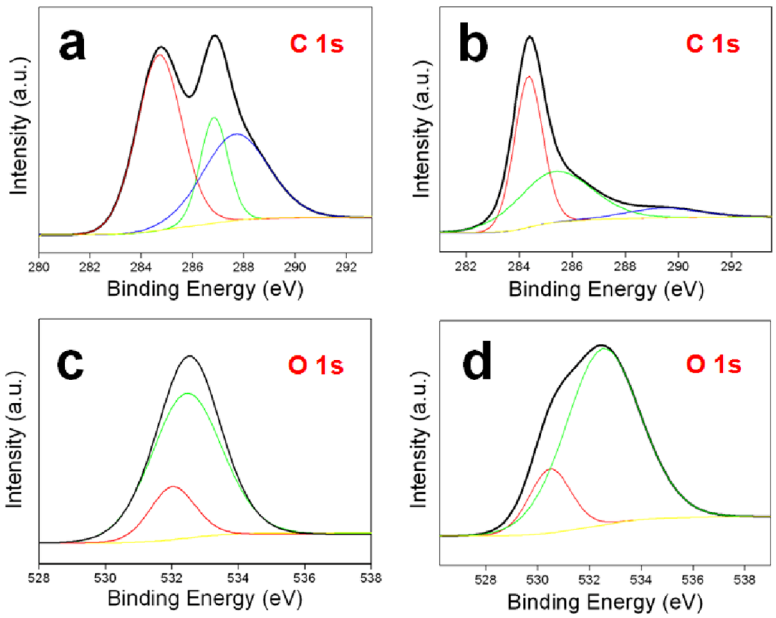

Figure 3 shows the nitrogen adsorption-desorption isotherms of RL-UCNTs. Generally, the nitrogen adsorption–desorption isotherms are used to characterise the specific surface areas and textural properties of the samples. As shown in Figure 3(a), the isotherms of RL-UCNTs correspond to the IUPAC type IV mesoporous structure and exhibit H3 hysteresis loop, indicating aggregates of plate-like particles. This result suggests that the porous properties come from aggregation of RL-UCNTs, which is also similar to that of graphene oxide. The pore size distribution of RL-UCNTs calculated using the BJH theory exhibited that pores of around 40 nm are well-developed. The specific surface area of RL-UCNTs is 288.0 m^2/g and most of them result from mesopores (282.0 m^2/g).

Figure 3 (a) Nitrogen adsorption and desorption isotherm curves of RL-UCNTs and (b) pore size distribution of RL-UCNTs (see online version for colours)

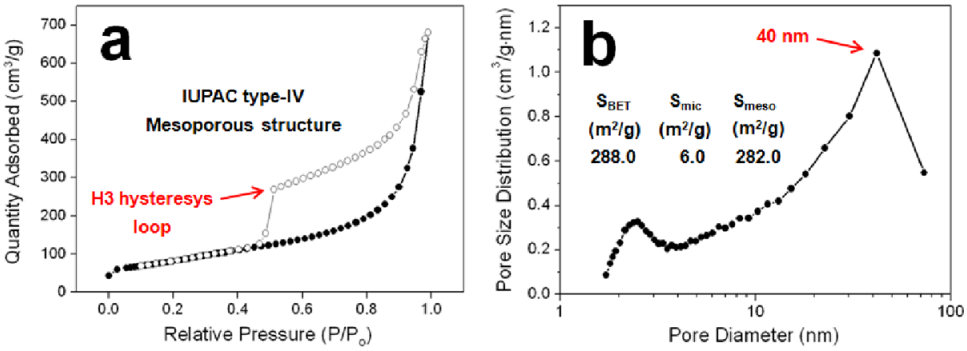

The electrochemical performance of RL-UCNTs was analysed using an aqueous electrolyte, 1 M H_2SO_4. Figure 4(a) shows the cyclic voltammograms of RL-UCNTs at a scan rate of 20 mV/s. The cyclic voltammogram curve exhibited a hump as well as a rectangular shape, indicating that the capacitive response results from the combination of electrical double-layer formation and redox reactions, which are related to the heteroatom functionalities of the materials. This result suggests that the oxygen functional groups greatly affect electrochemical performances of RL-UCNTs. Figure 4(b) shows the galvanostatic charge/discharge curves of RL-UCNTs at current densities of 0.5, 0.75 and 1 A/g. The discharge curves have linear slope from 1 to 0.5 V and the slopes are changed around 0.5 V, indicating pseudocapacitive effects by oxygen heteroatoms. This corresponds with the result of cyclic voltammogram. The specific capacitance of RL-UCNTs is 106 F/g at a current density of 0.5 A/g, and the specific capacitances were sharply decreased with an increase of the current density. At current densities of 5 and 10 A/g, the specific capacitances were 48 and 25 F/g, respectively. This result is due to low electro-conductivity of RL-UCNTs. However, the initial specific capacitance is higher than that of MWCNTs [8], because of pseducapacitive effects of oxygen functional groups. Also, electrochemical surface area of RL-UCNTs could be increased by unzipping MWCNTs, which could be confirmed from the electrochemical double-layer thickness in the cyclic voltammogram. After 5000 repetitive cycles at a scan rate of 50 mV/s in 1 M H_2SO_4 electrolytes, the specific capacitance was decreased to only 6.2% of the initial capacitance, demonstrating that RL-UCNTs have good cycle stability.

Figure 4 (a) Cyclic voltammogram of RL-UCNTs at a scan rate of 20 mV/s in 1 M H_2SO_4 electrolyte, (b) galvanostatic charge/discharge curves of RL-UCNTs at current densities of 0.5, 0.75 and 1 A/g, (c) specific capacitances of RL-UCNTs measured at different current densities and (d) variation of the specific capacitance of RL-UCNTs as a function of the cycle number measured at a scan rate of 50 mV/s (see online version for colours)

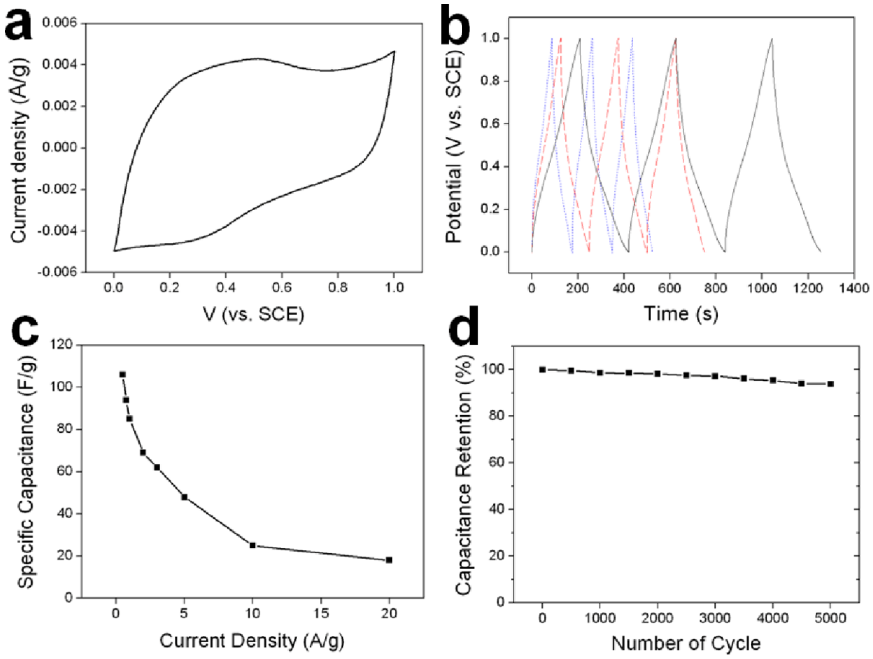

4 Conclusions

L-UCNTs were successfully prepared from MWCNTs and thermally treated at 600°C for 2 h to make RL-UCNTs with increased electrical properties. RL-UCNTs had mesoporous pore characteristics, and most of pores were around 40 nm. Their specific surface area was 288.0 m^2/g, and that of mesopores was 282.0 m^2/g. RL-UCNTs had numerous oxygen heteroatoms, and the heteroatoms greatly affect electrochemical performances of RL-UCNTs. RL-UCNTs exhibited a specific capacitance of 106 F/g at a current density of 0.5 A/g. Also, RL-UCNTs had a stable cycle life over 5000 cycles.

Acknowledgements

This research was supported by Basic Science Research Program through the National Research Foundation of Korea funded by the Ministry of Education (NRF-2013R1A1A2A10008534) and (NRF-2010-C1AAA001-0029018), and a grant from the Technology Development Program for Strategic Core Materials funded by the Ministry of Trade, Industry & Energy, Republic of Korea (Project No. 10047758).

References

1 Simon, P. and Gogotsi, Y. (2008) 'Materials for electrochemical capacitors', *Nat. Mater.*, Vol. 7, No. 11, pp.845–854.

2 Miller, J.R. and Simon, P. (2008) 'Electrochemical capacitors for energy management', *Science*, Vol. 321, No. 5889, pp.651–652.

3 Stoller, M.D., Park, S.J., Zhu, Y., An, J.H. and Ruoff, R.S. (2008) 'Graphene-based ultracapacitors', *Nano Lett.*, Vol. 8, No. 10, pp.3498–3502.

4 Pech, D., Brunet, M., Durou, H., Huang, P., Mochalin, V., Gogotsi, Y., Taberna, P.L. and Simon, P. (2010) 'Ultrahigh-power micrometre-sized supercapacitors based on onion-like carbon', *Nat. Nanotechnol.*, Vol. 5, No. 9, pp.651–654.

5 Kim, C. (2005) 'Electrochemical characterization of electrospun activated carbon nanofibres as an electrode in supercapacitors', *J. Power Sources*, Vol. 142, Nos. 1–2, pp.382–388.

6 Yun, Y.S., Shim, J.Y., Tak, Y.S. and Jin, H.J. (2012) 'Pseudocapacitive effects of N-doped carbon nanotube electrodes in supercapacitors', *Materials*, Vol. 5, No. 7, pp.1258–1266.

7 Yun, Y.S., Shim, J.Y., Tak, Y.S. and Jin, H.J. (2012) 'Nitrogen-enriched multimodal porous carbons for supercapacitors, fabricated from inclusion complexes hosted by urea hydrates', *RSC Advances*, Vol.2, No. 10, pp.4353–4358.

8 Frackowiak, E. and Beguin, F. (2002) 'Electrochemical storage of energy in carbon nanotubes and nanostructured carbons', *Carbon*, Vol. 40, No. 10, pp.1775–1787.

9 Geim, A.K. and Novoselov, K.S. (2007) 'The rise of graphene', *Nat. Mater.*, Vol. 6, No. 3, pp.183–191.

10 Stankovich, S., Dikin, D.A., Dommett, H.B., Kohlhaas, K.M., Zimney, E.J., Stach, E.A., Piner, R.D., Nguyen, S.B.T. and Ruoff, R.S. (2006) 'Graphene-based composite materials', *Nature*, Vol. 442, No. 7100, pp.282–286.

11 Yun, Y.S., Bae, Y.H., Kim, D.H., Lee, J.Y., Chin, I.J. and Jin, H.J. (2011) 'Reinforcing effects of adding alkylated graphene oxide to polypropylene', *Carbon*, Vol. 49, No. 11, pp.3553–3559.

12 Wang, X., Ouyang, Y., Jiao, L., Wang, H., Xie, L., Wu, J., Guo, J. and Dai, H. (2011) 'Graphene nanoribbons with smooth edges behave as quantum wires', *Nat. Nanotechnol.*, Vol. 6, No. 9, pp.563–567.

13 Shimizu, T., Haruyama, J., Marcano, D.C., Kosinkin, D.V., Tour, J.M., Hirose, K. and Suenaga, K. (2011) 'Large intrinsic energy bandgaps in annealed nanotube-derived graphene nanoribbons', *Nat. Nanotechnol.*, Vol. 6, No. 1, pp.45–50.

14 Han, M.Y., Ozyilmaz, B., Zhang, Y.B. and Kim, P.L. (2007) 'Energy band-gap engineering of graphene nanoribbons', *Phys. Rev. Lett.*, Vol. 98, No. 20, pp.206805(1)–206805(4).

15 Schniepp, H.C., Li, J.L., McAllister, M.J., Sai, H., Herrera-Alonso, M., Adamsou, D.H., Prud'homme, R.K., Car, R., Saville, D.A. and Aksay, I.A. (2006) 'Functionalized single graphene sheets derived from splitting graphite oxide', *J. Phys. Chem. B*, Vol. 110, No. 17, pp.8535–8539.

16 Yang, X., Dou, X., Rouhanipour, A., Zhi, L., Rader, H.J. and Mullen, K. (2008) 'Two-dimensional graphene nanoribbons', *J. Am. Chem. Soc.*, Vol. 130, No. 13, pp.4216–4217.

17 Kosynkin, D.V., Higginbotham, A.L., Sinitskii, A., Lomeda, J.R., Dimiev, A., Price, B.K. and Tour, J.M. (2009) 'Longitudinal unzipping of carbon nanotubes to form graphene nanoribbons', *Nature*, Vol. 458, No. 7240, pp.872–877.

18 Yun, Y.S., Bak, H.S. and Jin, H.J. (2010) 'Porous carbon nanotube electrodes supported by natural polymeric membranes for PEMFC', *Synth. Met.*, Vol. 160, Nos. 7–8, pp.561–565.

19 Mattevi, C., Eda, G., Agnoli, S., Miller, S., Mkhoyan, K.A., Celik, O., Mastrogiovanni, D., Granozzi, G., Garfunkel, E. and Chhowalla, M. (2009) 'Evolution of electrical, chemical, and structural properties of transparent and conducting chemically derived graphene thin films', *Adv. Funct. Mater.*, Vol. 19, No.16, pp.2577–2583.